

Perylene Bisimide Derivatives as Innovative Sensitizers for Photorefractive Composites

Thomas Schemme^a, Katharina Ditte^{a,b}, Evgenij Travkin^a, Wei Jiang^c,
Zhaohui Wang^c, and Cornelia Denz^a

^aInstitute of Applied Physics, Westfälische Wilhelms-Universität Münster,
Corrensstr. 2, Münster, Germany;

^bInstitute of Physics, Westfälische Wilhelms-Universität Münster,
Wilhelm-Klemm-Str. 10, Münster, Germany;

^cInstitute of Chemistry, Chinese Academy of Sciences,
Zhongguancun North First Street 2, Beijing, PR China

ABSTRACT

In photorefractive composites, we replace the commonly used fullerene derivative phenyl-C61-butyric acid methyl ester (PCBM) by the perylene bisimide dimer DiPBI. In samples, wherein poly-n-vinylcarbazole (PVK) is the charge transporting agent and 4-cyano-4-n-pentylbiphenyl (5CB) the nonlinear optical unit, we observe dramatic enhancements in the overall performance of the composites. When we replace PVK by *N,N'*-diphenyl-*N,N'*-bis(3-methylphenyl)-[1,1'-biphenyl]-4,4'-diamine (TPD) doped polystyrene (PS), the internal photocurrent efficiency is further improved by a factor 11.

Keywords: Photorefractive composites, conductive organic materials, charge transport, two-beam coupling

1. INTRODUCTION IN PHOTOREFRACTIVE COMPOSITES

Since the first observation of the photorefractive (PR) effect in an inorganic crystal by Ashkin et al.,¹ many applications that make use of this process have been developed. Holographic data storage,² novelty filters,³ and beam couplers^{4,5} can be mentioned as the most prominent ones. But, due to the fact that the growth processes of photorefractive inorganic crystals are cost intensive, complex, the crystals are only available in rather small dimensions, and their PR performance is rather slow, they are not suitable for real-time mass market devices. To find an alternative, large research efforts have been made to improve the performance of organic photorefractive materials during the last 20 years. Out of several approaches for organic PR materials, the ansatz of PR composites turned out to be the most promising one.⁶ Especially if large area devices, fast response times, or easy and cheap fabrication are needed, PR composites outmatch their inorganic counterparts. Due to these properties, photorefractive composites are ideal candidates to be employed as fast storage devices, optical beam couplers,⁷ tomographs for living tissue,⁸ and holographic 3d displays.⁹

The photorefractive effect describes a reversible refractive index change that is caused by inhomogeneous illumination of the material.¹⁰ The underlying phenomena of this process are photoconductivity and the electro-optic effect. Illumination of a photorefractive composite with a light pattern leads to excitation of absorbing sensitizer molecules in the regions of high light intensity. Under the influence of an applied external electric field, these excitons are separated, and the mobile holes move through the (polymeric) hole transporter, while the immobile electrons remain in the excited sensitizer molecules. In the dark regions, holes can be trapped by energetic inhomogeneities and hence the redistributed charges lead to the formation of a space-charge field. Nonlinear optical units, e.g., liquid crystals that provide the electro-optic effect, translate the space-charge field into the desired refractive index change.¹¹

Further author information: (Send correspondence to T.S.)

T.S.: E-mail: t.schemme@uni-muenster.de, Telephone: +49 (0) 251 83 36154

There are several challenges in the optimization process of photorefractive composites. One major issue, especially when real-time applications are considered, is the time until the refractive index change occurs, also called photorefractive speed. Another issue is the light sensitivity of the composition which has to be tailored to the operating wavelength of the desired application. Both issues can be faced by an optimization of the photoconductivity, which is a combined process of charge generation and transport.¹² So, the simplest way to improve both processes at once is to find a highly efficient sensitizer that strongly absorbs light in the desired wavelength region. Optimization of the charge transporting material will only lead to an enhanced mobility and not increase the sensitivity. But this can be considered as a second step to further increase the photoconductivity, when an appropriate sensitizer is found. This step will also offer the possibility to lower the applied electric field, that is usually in the $E_{\text{ext}} = 70 \text{ V } \mu\text{m}^{-1}$ region.

In comparison with a modified version of the well-known composition^{13,14} of the electro-optic liquid crystal 4-cyano-4-n-pentylbiphenyl (5CB), the conductive polymer poly-n-vinylcarbazole (PVK) and C_{60} (5CB:PVK: C_{60}), where the fullerene is replaced by its derivative phenyl-C61-butyric acid methyl ester (PCBM), we replace PCBM by the perylene bisimide dimer DiPBI to enhance the charge generation and therefore the photoconductivity.¹⁵ DiPBI provides strong electron affinity, air stability, and strong and broad absorption in the whole visible range. In a second step, we replace PVK by *N,N'*-diphenyl-*N,N'*-bis(3-methylphenyl)-[1,1'-biphenyl]-4,4'-diamine (TPD) doped polystyrene (PS) as charge transporting agent to further improve the photoconductivity¹⁶⁻¹⁸ and reduce the applied electric field.

2. SAMPLE PREPARATION AND EXPERIMENTAL TECHNIQUES

For the analysis of the influence of DiPBI on the photoconductive and photorefractive properties of the compositions, we fabricate samples with the same molecular amounts of PCBM and DiPBI, respectively. This procedure results in a molecular ratio of PVK, 5CB, and sensitizer of 0.983:98.881:0.136 mol%, and weight ratios of 59.69:40.11:0.20 wt% (PVK:5CB:PCBM), as used by Zhang and Singer,¹³ and 59.60:40.05:0.35 wt% (PVK:5CB:DiPBI), assuming PVK to be 37500 g mol^{-1} averaged. As DiPBI shows a strong absorption, also samples with reduced sensitizer amount are prepared. For the investigation of PS:TPD as charge transporter, a weight ratio of 59.80:40.18:0.02 wt% (PVK:5CB:DiPBI) is chosen and PVK is replaced by PS:TPD in a 80.00:20.00 wt% ratio. All components except DiPBI are bought from Aldrich and used without further purifi-

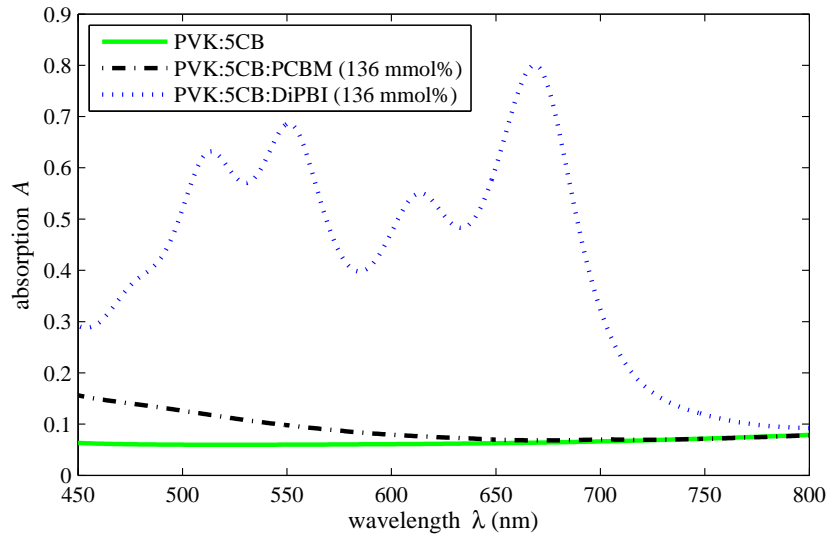


Figure 1. Absorption spectra of an unsensitized sample, and of samples containing PCBM or DiPBI as sensitizer.

cation. The synthesis of DiPBI is described in a previous report.¹⁹ For sample preparation, all components are dissolved in chloroform at the desired ratio. After this step, the composite is dropped onto indium tin oxide

(ITO) coated glass substrates, and annealed in an oven at 55 °C for four hours to remove the residual solvent. Finally, a $d = 50 \mu\text{m}$ thick spacer foil and the second ITO coated glass is added and the sample is melt-pressed at 90 °C.

Absorption spectra measured with a *Jasco V-530 UV/VIS* spectrometer are depicted in Figure 1 and Figure 2. The spectra in Figure 1 clearly illustrate the strong and broad absorption of DiPBI in contrast to PCBM. In addition, absorption at a wavelength of 532 nm is investigated by measuring of the transmitted intensity of a laser beam assuming the glass non absorbing. Employing a modified version of the Beer-Lambert law,²⁰ absorption coefficients of the sensitized samples at a wavelength of 532 nm are calculated by $\alpha = A/d$ to $\alpha_{\text{PCBM}} = (9 \pm 1) \text{ cm}^{-1}$ and $\alpha_{\text{DiPBI}} = (53 \pm 3) \text{ cm}^{-1}$. Here, A is the measured absorption and d is the sample thickness. As illustrated in Figure 2, the DiPBI doped PS:TPD sample provides the strongest absorption, while

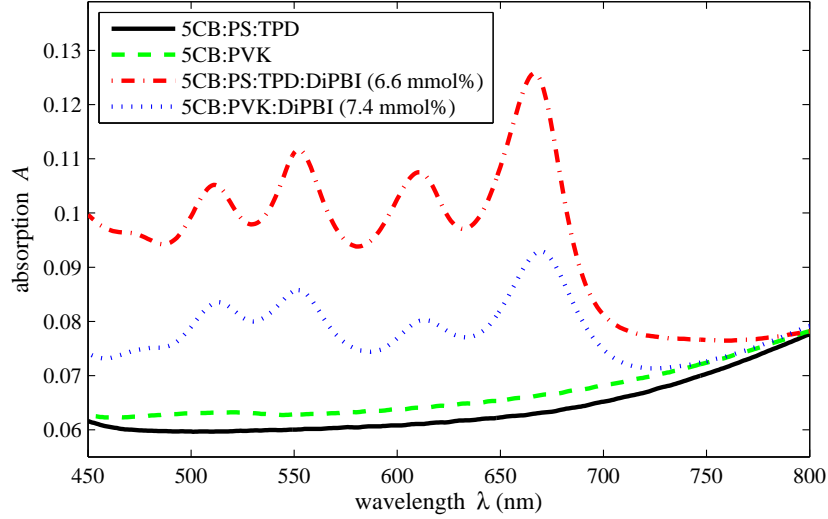


Figure 2. Absorption spectra of samples containing PS:TPD or PVK as hole transporter, and with and without sensitizer, respectively.

the unsensitized version possesses the weakest absorption. Although there are small differences, the absorption of the composites is clearly governed by the sensitizer DiPBI. The absorption coefficients of the sensitized composites at 532 nm are $\alpha_{\text{PS:TPD}} = (20 \pm 1) \text{ cm}^{-1}$ and $\alpha_{\text{PVK}} = (16 \pm 1) \text{ cm}^{-1}$.

The photoelectric properties of the composites are investigated by measurements of the photocurrent I_{ph} with a *Keithley 6485 picoammeter* under homogeneous illumination of the samples with an intensity of $W = 16 \text{ mW cm}^{-2}$ at a wavelength of 532 nm, an applied external electric field E_{ext} , and a fixed electrode area of $a = 39 \text{ mm}^2$. During the measurement procedure, the dark current I_{dark} as well as the current under illumination I are characterized. The photocurrent I_{ph} is given by $I_{\text{ph}} = I - I_{\text{dark}}$. Then the photoconductivity is calculated by

$$\sigma_{\text{ph}} = \frac{I_{\text{ph}}}{a E_{\text{ext}}}. \quad (1)$$

Employing the absorption coefficients of the samples, the internal photocurrent efficiency ϕ_{int} , which is given by

$$\phi_{\text{int}} = \frac{\sigma_{\text{ph}} E_{\text{ext}} h \nu}{e \alpha d W}, \quad (2)$$

is calculated to eliminate the influence of small differences in the absorption properties of the samples.²¹ Here h is Planck's constant, ν the frequency of light, e the elementary charge, α the absorption coefficient of the particular sample, and d the sample thickness.

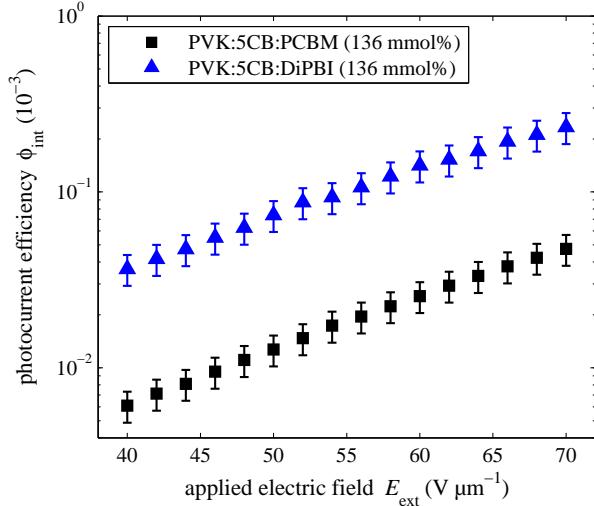


Figure 3. Internal photocurrent efficiencies for samples with equal content of the sensitizers PCBM and DiPBI, respectively.

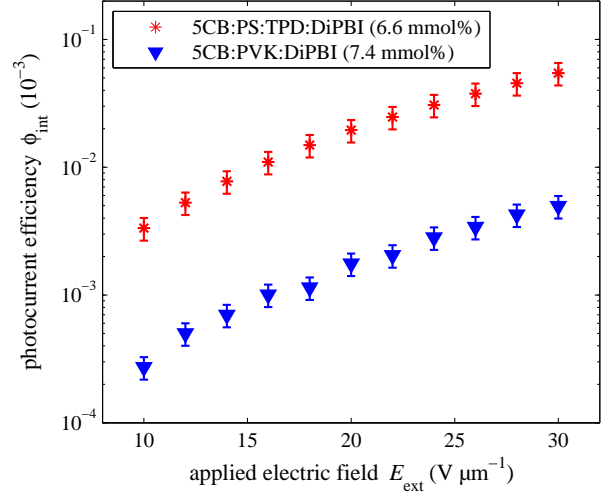


Figure 4. Internal photocurrent efficiencies for DiPBI-sensitized samples with hole transporters PVK and PS:TPD, respectively.

The photorefractive qualities are investigated for different applied electric fields by the well-known two-beam coupling technique.²² We illuminate the sample with two interfering laser beams, each with an intensity of $W_{1,2} = 8 \text{ mW cm}^{-2}$. The sample normal is tilted with respect to beam 1 by 40° and beam 2 by 60° , resulting in a grating spacing of $2 \text{ }\mu\text{m}$, if a refractive index of $n = 1.7$ is assumed. The energy transfer between both p-polarized beams is given by the gain coefficient Γ , calculated with

$$\Gamma = \frac{1}{L} [\ln(\gamma b) - \ln(1 + b - \gamma)], \quad (3)$$

where b is the intensity ratio between the beams in front of the sample and L the optical path length inside the sample. The gain γ is measured after propagation through the sample via a photo diode and is described by the expression $\gamma = W_1(W_2 > 0)/W_1(W_2 = 0)$. The PR speed is the reciprocal value of the fast time constant achieved by fitting a biexponential decay function on the curves of the PR response.

3. ENHANCED PHOTOCONDUCTIVE AND PHOTOREFRACTIVE RESPONSE

The investigated photocurrents are transferred into internal photocurrent efficiencies by application of the equations (1) and (2). The figures 3 and 4 illustrate ϕ_{int} in dependence on the applied electric field E_{ext} . As depicted in Figure 3, the curves of both compositions rise almost linear. Further, the values of ϕ_{int} for the DiPBI-sensitized samples at $E_{\text{ext}} = 70 \text{ V }\mu\text{m}^{-1}$ are about 4 times larger than for the PCBM-sensitized samples. This behavior can clearly be attributed to an enhanced charge generation of DiPBI. The photocurrent measurements depicted in Figure 4 are investigated at lower electric fields to avoid electric breakdown and with a 94% reduced sensitizer concentration. The experiment reveals stronger dark- and photocurrents for the PS:TPD comprising samples, which indicate a lower trap concentration in this composition. These results can be directly transferred to the photo- and dark conductivities, as their relation is linear. Considering the data in Figure 4 of the sample with PS:TPD as hole transporter, an increase of ϕ_{int} at an applied electric field of $E_{\text{ext}} = 30 \text{ V }\mu\text{m}^{-1}$ by a factor 11 is observed. This enhancement is attributed to a much better charge separation between DiPBI and TPD, compared to DiPBI and PVK, and the high hole mobility in TPD. These properties of the PS:TPD-based system allow for effective charge generation and transport at reduced applied electric fields. In comparison, the data of the PCBM-sensitized sample (\blacksquare in Figure 3) and the DiPBI-sensitized sample ($*$ in Figure 4) are in the same order of magnitude, although lower electric fields are applied to the DiPBI-sample.

The two-beam coupling experiment reveals the photorefractive properties of the composites. For all samples, an increase of the light intensity of one beam is observed, while the intensity of the other beam decreases. When

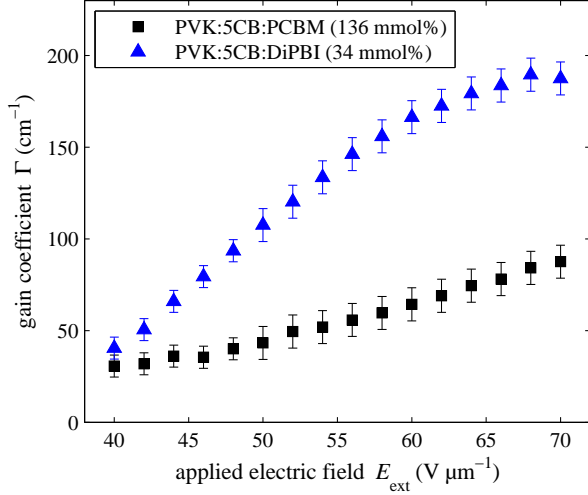


Figure 5. Gain coefficient in dependence on applied electric field for samples with PCBM and 75% reduced content of DiPBI, respectively.

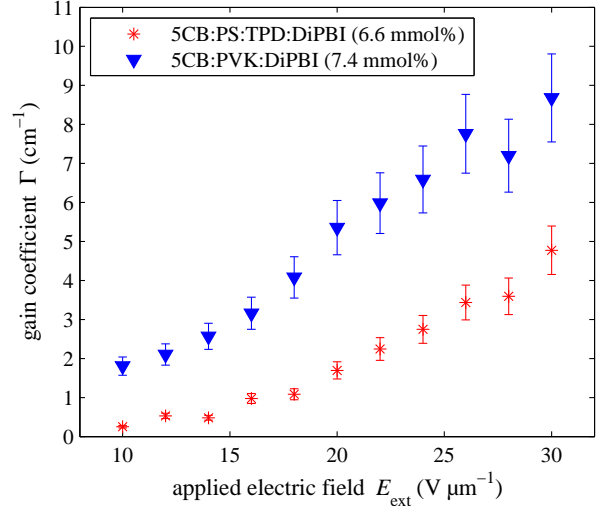


Figure 6. Gain coefficient in dependence on applied electric field for DiPBI-sensitized samples with hole transporters PVK and PS:TPD, respectively.

the direction of the applied electric field is changed, the direction of the energy coupling also changes. Applying equation (3), we calculate the gain coefficient Γ of the two-beam coupling. The figures 5 and 6 and illustrate the dependence of Γ on the applied electric field. Figure 5 clearly depicts the superior two-beam coupling performance of DiPBI in samples with 75% reduced content, compared to the standard PCBM-sensitized samples. Additionally to the increased gain coefficient by a factor 2, also the photorefractive speed is dramatically enhanced. We observe a 39 times faster PR speed in the DiPBI samples with 75% reduced content, compared to the standard PCBM samples.¹⁵

Although the photoconductivity and internal photocurrent efficiency of PS:TPD comprising samples are much larger than in PVK comprising samples, this relation is reversed for Γ , as depicted in Figure 6. The gain for the PVK containing composite is about 1.8 times larger. The lower performance of the PS:TPD samples is explained by a too low trap concentration in the samples. For a strong space-charge field resulting in a strong and fast PR performance, there has to be enough trapping of redistributed charges. High dark currents and therefore low trapping inevitably lead to low photorefractivity because of weak space-charge fields. An enhancement of the contrast between photo- and dark conductivity is necessary to further improve PR properties of the composites. In the PS:TPD system, this may be realized by a reduction of the TPD content or doping with a further component to incorporate more traps. These steps will lower the mobility of the holes and so the photoconductivity will also be lowered, resulting in the need of higher applied fields. Therefore, the relation between the photo- and dark conductivity has to be well-balanced.

4. CONCLUSION

We incorporate diperylene bisimide into photorefractive composites and employ absorption spectroscopy, photocurrent measurements and two-beam coupling for the characterization of the composites. Beside very strong absorption, the DiPBI-sensitized samples also provide dramatic enhancements of the photoconductivity, compared to PCBM-sensitized samples. PR speed and gain coefficient are also improved in DiPBI-based composites that comprise PVK as charge transporter. Due to a strongly reduced trapping of redistributed charges, the PR gain coefficient in DiPBI-sensitized composites with PS:TPD as charge transporter is lower than in PVK comprising composites.

ACKNOWLEDGMENTS

Financial support by Deutsche Forschungsgemeinschaft within the SFB/Transregio TRR 61 is gratefully acknowledged.

REFERENCES

- [1] Ashkin, A., Boyd, G. D., Dziedzic, J. M., Smith, R. G., Ballman, A. A., Levinstein, J. J., and Nassau, K., "Optically-Induced Refractive Index Inhomogeneities in LiNbO_3 and LiTaO_3 ," *Appl. Phys. Lett.* **9**(1), 72–74 (1966).
- [2] Denz, C., Müller, K.-O., Heimann, T., and Tschudi, T., "Volume holographic storage demonstrator based on phase-coded multiplexing," *IEEE J. Sel. Topics in Quantum Electron.* **4**(5), 832–839 (1998).
- [3] Krishnamachari, V. V., Grothe, O., Deitmar, H., and Denz, C., "Novelty filtering with a photorefractive lithium–niobate crystal," *Appl. Phys. Lett.* **87**(7), 071105 (2005).
- [4] Cronin-Golomb, M., Kong, H., and Krolikowski, W., "Photorefractive 2-beam coupling with light of partial spatiotemporal coherence," *J. Opt. Soc. Am. B* **9**(9), 1698–1703 (1992).
- [5] Shumelyuk, A., Ruediger, A., Schirmer, O., Hilling, B., Dieckmann, V., Brüning, H., Schemme, T., Imlau, M., and Odoulov, S., "Temperature Dependence of Photorefractive Response of $\text{Sn}_2\text{P}_2\text{S}_6$," *J. Holography Speckle* **5**, 290–293 (2009).
- [6] Moerner, W., Grunnet-Jepsen, A., and Thompson, C., "Photorefractive Polymers," *Annu. Rev. Mater. Sci.* **27**, 585–623 (1997).
- [7] Ostroverkhova, O. and Moerner, W., "Organic photorefractives: Mechanisms, materials, and applications," *Chem. Rev.* **104**(7), 3267–3314 (2004).
- [8] Salvador, M., Prauzner, J., Köber, S., Meerholz, K., Turek, J. J., Jeong, K., and Nolte, D. D., "Three-dimensional holographic imaging of living tissue using a highly sensitive photorefractive polymer device," *Opt. Express* **17**(14), 11834–11849 (2009).
- [9] Blanche, P.-A., Bablumian, A., Voorakaranam, R., Christenson, C., Lin, W., Gu, T., Flores, D., Wang, P., Hsieh, W.-Y., Kathaperumal, M., Rachwal, B., Siddiqui, O., Thomas, J., Norwood, R. A., Yamamoto, M., and Peyghambarian, N., "Holographic three-dimensional telepresence using large-area photorefractive polymer," *Nature* **468**(7320), 80–83 (2010).
- [10] Günter, P. and Huignard, J.-P., [*Photorefractive Materials and their Applications 1: Basic Effects*], Springer (2006).
- [11] Moerner, W. E. and Silence, S. M., "Polymeric photorefractive materials," *Chem. Rev.* **94**(1), 127–155 (1994).
- [12] Steenwinckel, D. V., Hendrickx, E., and Persoons, A., "Dynamics and steady-state properties of photorefractive poly(N-vinylcarbazole)-based composites sensitized with (2,4,7-trinitro-9-fluorenylidene)malononitrile in a 0–3 wt % range," *J. Chem. Phys.* **114**(21), 9557–9564 (2001).
- [13] Zhang, J. and Singer, K., "Homogeneous photorefractive polymer/nematogen composite," *Appl. Phys. Lett.* **72**(23), 2948–2950 (1998).
- [14] Ostroverkhova, O. and Singer, K., "Space-charge dynamics in photorefractive polymers," *J. Appl. Phys.* **92**(4), 1727–1743 (2002).
- [15] Ditte, K., Jiang, W., Schemme, T., Denz, C., and Wang, Z., "Innovative Sensitizer DiPBI Outperforms PCBM," *Adv. Mater.* **accepted** (2012).
- [16] Jung, G. B., Yoshida, M., Mutai, T., Fujimura, R., Ashihara, S., Shimura, T., Araki, K., and Kuroda, K., "High-speed TPD-based Photorefractive Polymer Composites," *Sen'i Gakkaishi* **60**(6), 193–197 (2004).
- [17] Mohan, S. R. and Joshi, M., "Field dependence of hole mobility in TPD-doped polystyrene," *Solid State Commun.* **139**(4), 181–185 (2006).
- [18] Schemme, T., Travkin, E., Ditte, K., Jiang, W., Wang, Z., and Denz, C., "TPD Doped Polystyrene as Charge Transporter in DiPBI Sensitized Photorefractive Composites," *Opt. Mater. Express* **submitted** (2012).
- [19] Qian, H., Wang, Z., Yue, W., and Zhu, D., "Exceptional Coupling of Tetrachloroperylene Bisimide: Combination of Ullmann Reaction and C–H Transformation," *J. Am. Chem. Soc.* **129**(35), 10664–10665 (2007).

- [20] Swinehart, D. F., "The Beer-Lambert Law," *J. Chem. Educ.* **39**(7), 333 (1962).
- [21] Däubler, T. K., Bittner, R., Meerholz, K., Cimrová, V., and Neher, D., "Charge carrier photogeneration, trapping, and space-charge field formation in PVK-based photorefractive materials," *Phys. Rev. B* **61**(20), 13515–13527 (2000).
- [22] Yeh, P., "Two-Wave Mixing in Nonlinear Media," *IEEE J. Quantum. Electron.* **25**(3), 97–132 (1989).